Published in final edited form as:
Eur J Immunol. 2012 April ; 42(4): 1038–1043. doi:10.1002/eji.201142193.

Overexpression of Snai3 suppresses lymphoid- and enhances myeloid-cell differentiation

Timothy Dahlem[1], **Scott Cho**[2], **Gerald J. Spangrude**[2], **Janis J. Weis**[1], and **John H. Weis**[1]

[1]Division of Cell Biology and Immunology, Department of Pathology, University of Utah School of Medicine, Salt Lake City, UT, USA

[2]Division of Hematology, Department of Internal Medicine, University of Utah School of Medicine, Salt Lake City, UT, USA

Abstract

The altered expression of transcription factors in hematopoietic stem cells and their subsequent lineages can alter the development of lymphoid and myeloid lineages. The role of the transcriptional repressor Snai3 protein in the derivation of cells of the hematopoietic system was investigated. Snai3 is expressed in terminal T-cell and myeloid lineages, therefore, we chose to determine if expressing Snai3 in the early stages of hematopoietic development would influence cell-lineage determination. Expression of Snai3 by retroviral transduction of hematopoietic stem cells using bone marrow chimera studies demonstrated a block in lymphoid-cell development and enhanced expansion of myeloid-lineage cells. Analysis of Snai3-expressing hematopoietic precursor cells showed normal numbers of immature cells, but a block in the development of cells committed to lymphoid lineages. These data indicate that the overexpression of Snai3 does alter bone marrow cell development and that the identification of genes whose expression is altered by the presence of Snai3 would aid in our understanding of these developmental pathways.

Keywords

Animal models; Bone marrow; Cell differentiation; Transcription; Transcription factors

Introduction

In vertebrate species there are four members of the Snail superfamily: Snai1, Snai2, Snai3, and Scratch [1]. Snail family members function as transcriptional repressors by their N-terminal-repressor domain or by sequence-specific binding to DNA by their C-terminal zinc finger domain [1, 2]. Mammalian family members have a conserved N-terminal SNAG (Snail/Gfi-1) domain that interacts with corepressors and is either required for, or augments repression [2–4]. The DNA binding, C_2H_2 zinc fingers of the Snail proteins are similar and conserved; the zinc fingers of the mouse Snai1, Snai2, and Snai3 proteins are ~ 60–95% identical in amino acid sequence [2, 3]. Snail family members bind to E box consensus sites of CAGGTG (or CANNTG) [3] with the mouse Snai3 protein showing specificity for CACCA/TG/T [5].

Full correspondence: Dr. John Haynes Weis, University of Utah, Department of Pathology, 15 North Medical Drive East, Salt Lake City, Utah 84112, USA, Fax: +1-801-581-4517, john.weis@path.utah.edu.

Conflict of interest: The authors declare no financial or commercial conflict of interest.

In the mouse, Snai1 and Snai2 have been associated with embryogenesis and epithelial-mesenchymal transition [6–10]. Snai2 is a downstream effector of the stem cell factor (SCF)/c-Kit signaling pathway and Snai2-knockout mice have a similar phenotype to the SCF (*sl*) and c-Kit (w/w^v) mutant mice [11]. Snai2$^{-/-}$ mice have atrophied thymus, however, other hematopoietic lineages develop normally in these mice [11]. Overexpression of Snai1 also causes an atrophied thymus, but peripheral blood CD4$^+$ and CD8$^+$ T-cell populations are unaffected [12]. Forced expression of either Snai1or Snai2 can lead to B-cell and myeloid leukemias [12–14].

Snai3 has been shown to actively repress transcription [3]. Snai3 expression has been reported in skeletal muscle, thymus, and myeloid cells [3, 5, 15, 16]. Human Snai3 (SNAI3) has been identified in silico and contains the same SNAG and zinc finger domains as the mouse protein [17]. To elucidate the function of mouse Snai3, we adopted a gain of function approach to determine if the expression of Snai3 in hematopoietic stem cell (HSC) precursors would alter the derivation of mature end-stage lineage cells. In this report, we demonstrate that constitutive expression of Snai3 in early bone marrow (BM) lineages resulted in a block in lymphoid-development concomitant with an expansion of myeloid lineages suggesting that Snai3 repression of target genes in differentiating myeloid and lymphoid cells had opposite effects upon their maturation.

Results and discussion

Snai3 retroviral bone marrow transduction and reconstitution of irradiated animals

We constructed a Snai3-expressing retrovirus vector that could be used to infect BM HSCs that would give rise to hematopoietic cell lineages. We utilized the pBMN-1 green fluorescent protein (GFP) retrovirus vector (Empty-RV) by cloning the coding sequence of Snai3 just upstream of the internal ribosome entry site (IRES) site and GFP gene, producing a bicistronic transcript such that every cell expressing GFP should also produce Snai3 (Snai3-RV) (Fig. 1A). The Plat-E virus packaging line transfected with control Empty-RV or Snai3-RV showed GFP protein expression for both virus constructs but Snai3 protein only upon Snai3-RV transfection (Fig. 1D). Supernatants from these packaging line cultures were used to transduce HSC (Fig. 1B and D). Efficiency of transduction with Empty-RV (top plot) or Snai3-RV (bottom plot) virus averaged about 40–50% of the culture. HSC from B6.SJL mice that express the polymorphic hematopoietic CD45.1 marker (donor mice) were infected with the Empty-RV and Snai3-RV supernatants and transplanted into irradiated C57BL/6 mice (recipient mice) that possess the CD45.2 polymorphic hematopoietic marker. The protocol allowed each cell to be identified as donor or recipient origin based on CD45 surface expression. RV-chimeric mice had between 75 and 87% reconstitution with the CD45.1 donor cells in the peripheral blood mononuclear cells (PBMCs) (Fig. 1C); additional experiments also ranged from 75 to 95% reconstitution (data not shown). The GFP histograms of the PBMCs of RV-chimeric mice show that about 38% of cells in the Snai3-RV-transduced mouse expressed high levels of GFP (and Snai3) while about 18% of the Empty-RV-transduced mouse expressed high levels of GFP (but no Snai3) (Fig. 1C). The efficiency of virus transduction and reconstitution varied but averaged about 35% total GFP$^+$ cells for Snai3-RV and 25% for Empty-RV constructs. The percentage of CD45.1 donor cells and GFP$^+$ cells in these RV-chimeric mice remained constant beyond 12 weeks post-transplant indicative of long-term stem cell reconstitution.

Snai3 constitutive expression inhibits lymphocyte and promotes myeloid development

To determine if the constitutive expression of *Snai3* affected the development of hematopoietic lineages, PBMCs obtained from irradiated mice reconstituted with BM transduced with either the Empty-RV or Snai3-RV vectors were stained with lineage surface

markers 8 weeks postreconstitution and analyzed by fluorescence-activated cell sorter (FACS) [18]. Each PBMC lineage was analyzed as a total PBMC population (left set of panels) and then gated into three subsets (GFP Negative, GFP Low, and GFP High) (See Fig. 1C) [19, 20]. As shown in Fig. 2A and B, in comparing a single set of Empty-RV and Snai3-RV animals, virtually no GFP^+ Snai3-expressing B cells were found in the Snai3-RV samples (3%) while GFP^+ B cells were evident in the Empty-RV animals (45%). Conversely, GFP^+ Snai3-expressing cells of the myeloid lineage were found in the Snai3-RV animals (47%) similar to that seen for GFP^+ myeloid cells from the empty-RV animal (36%). In order to quantify these data, $n = 9$ different Empty-RV mice and $n = 7$ Snai3-RV mice were analyzed (Fig. 2C). The percentages of total $CD4^+$ and $CD8^+$ T cells, $B220^+CD19^+$ B cells, $GR1^+CD11b^+$ granulocytes, and $CD11b^+$ monocytes were the same between the two sets of samples except for a slight expansion in total $CD11b^+$ monocytes in the Snai3-RV samples (total PBMCs). The Snai3-RV infected lineages were virtually devoid of lymphoid cells ($CD4^+$ and $CD8^+$ T cells, and $B220^+$ CD19 B cells: GFP High Subset) that were clearly present in the Empty-RV animals (GFP High Subset) although the depression of B-cell development in the Snai3-overexpressing cells appears to be more complete than that of the T-cell lineages. Cells expressing the Snai3-RV were primarily of the myeloid lineages defined by the GR1 and CD11b markers. Lymphoid lineages within the Snai3-RV mice were present; however, but only within the noninfected population (GFP Negative and GFP Low subsets). Thus the presence of Snai3 during bone marrow cell differentiation either poisons lymphocyte development or dramatically enhances the development of myeloid lineages.

Constitutive expression of Snai3 does not alter development of early stem cell lineages

The previous figure demonstrated the effect of Snai3 expression on the presence of end stage cells but did not indicate at what point in hematopoietic cell differentiation the function of Snai3 is critical. To address this question, we sought to determine if the expression of *Snai3* in HSC altered the development of early progenitor populations. After depletion of the lineage-positive fraction and analyzing the remaining cells (Lin^-) with antibodies specific for c-Kit and Sca-1 surface markers, BM progenitors were divided into four progressively more differentiated and mature populations [21–25]. Specifically, four gates were used to analyze Sca-1 and c-Kit populations (Fig. 3, left panels), starting with the least to the most differentiated: Gate 1- c-$Kit^+Sca\text{-}1^+$, Gate 2- c-$Kit^+Sca\text{-}1^{Int}$, Gate 3- c-$Kit^{Int}Sca\text{-}1^{Int}$, and Gate 4- c-$Kit^+Sca\text{-}1^-$ [21, 23, 26]. The percentage of cells in each gate is shown as a number next to each box in the Lin^- BM plots.

Analyzing the gated populations for GFP expression (right panels) showed that the populations in all four gates were virtually identical with no absence or expansion in each gate when comparing Empty-RV and Snai3-RV mice, and in comparing with wild-type (WT) BM. The lack of alteration in any one of the four gated progenitor populations indicates that the blockade of lymphocyte differentiation and expansion of the myeloid lineage occurs in more mature progenitor stages of these lineages.

Additional experiments on such mice indicated no GFP^{High} cells were found in the thymus of Snai3-RV mice (data not shown). GFP^{High} cells are found in the BM of Snai3-RV (and Empty-RV) mice; however, the GFP^{High} cells in Snai3-RV mice do not express B220, CD43, or IgM that are indicative of the first stages (pro-B and pre-B) of B-cell development (data not shown). Thus the blockade in differentiation of maturing T and B cells in the Snai3-expressing HSC occurs between the c-Kit^+Sca^- stage and the more mature common lymphoid progenitor population.

Concluding remarks

The data presented in this report indicate that the expression of Snai3 in bone marrow progenitors alters neither the maintenance of the stem cells nor the early stages of stem-cell differentiation but does dramatically skew the production of cells committed to the lymphoid or myeloid lineages. The Snai3 protein could alter these maturation profiles either through the repressor function of the SNAG domain of the protein, or by competing with endogenous transcriptional regulators for binding to E box sites. The identification of genes whose expression is influenced by the presence of Snai3 in these precursor populations may provide key insight into the regulation of differentiation of myeloid- and lymphoid-precursor cells.

Materials and methods

Animals

Animals were housed in the Animal Resource Center (University of Utah Health Science Center, Salt Lake City, UT) according to the guidelines of the National Institutes of Health. C57BL/6 and B6.SJL-Ptprc Pepc/BoyJ were obtained from The Jackson Laboratories. C57BL/6CrSlc-Tg(ACTb-EGFP)OsbC14-Y01-FM131 mice ubiquitously expressing GFP were utilized [27].

Retroviral constructs/transfection

The pBMN-1-GFP retrovirus was obtained from Addgene (plasmid 1736). The coding sequence of Snai3 (base pair (bp) 79–942 of NM 013914.2) was cloned into the Bam HI and XhoI sites of the vector. The Snai3 encoding cDNA was obtained by RT-PCR amplification of mouse thymus cDNA using 5′-CGGATCCATGC CGCGCTCCTTCCTGGTGA and 5′-GCTCGAGCTAGGGGCCAGGAC AGCAGC oligonucleotides. PCR amplification was performed using Platinum pfx (Invitrogen, Grand Island, NY, USA). PCR amplification was 55°C annealing (30 s), 68°C extension (2 min) and 95°C denaturing (30 s) for 40 cycles. After subcloning the sequence was confirmed to match that of the reference sequence of NM 013914.2. Plat E cells were grown in stem cell media (SCM): Dulbecco's modified Eagle'smedium (DMEM) supplemented with 15% FCS, P/S, 1 μg/mL puromycin (Sigma, St. Louis, MO, USA), and 10 μg/mL blasticidin (Sigma) except during virus production when antibiotics were subtracted [28]. Retroviral vectors were transfected into the Plat E packaging cell line using Fugene HD reagent (Roche, Pleasanton, CA, USA) at a 6:1 ratio. Cells were incubated at 37°C for 24 h then switched to 32°C for virus production in fresh media. Supernatant was collected and filtered through a 0.45 μm filter prior to use in transduction.

Retroviral transduction of bone marrow

B6.SJL were injected with 300 μL 10 mg/mL 5′ fluorouracil (Sigma) in PBS [29]. Four days later their BM was collected and cultured with RBC in SCM with 100 ng/mL SCF (Sigma), 20 ng/mL IL-6 (Sigma), and 10 ng/mL IL-3 (Sigma) at 5–6 × 10^6 cell/mL for 2 days at 37°C. Stem cell cultures were collected and red blood cell (RBC) lysed with ammonium chloride potassium (ACK). Remaining cells were resuspended in 7.5 mL filtered retroviral supernatant, 2.5 mL SCM, 4 μg/mL polybrene (Sigma), and fresh cytokines into six well plates treated with human fibronectin (Sigma) for 4 h at room temperature. Cultures were transduced by spinoculation at 1800 rpms and 37°C for 2 h. Cultures were incubated at 37°C for 24 h and then retransduced with fresh virus supernatant for another 24 h. Cultures were collected, washed twice in PBS, resuspended in PBS, and retinal orbitally injected into irradiated C57BL/6 mice. C57BL/6 mice were irradiated with one lethal dose of 950 rads 24 h prior to reconstitution.

FACS analysis

PBMCs were collected by submandular bleeds into heparin (Sigma) treated tubes. RBCs were precipitated with 20 mg/mL Dextran T500 (Amersham Pharmacia Biotech, Piscataway, NJ, USA) in PBS for 30 min at 37°C. Supernatants were collected, spun, and remaining RBC were lysed with ACK. Cells were washed twice with staining buffer (PBS + 0.5% BSA) before staining with CD45.1-PE (eBioscience A20, San Diego, CA, USA) and CD45.2-PerCP-Cy5.5 (eBioscience 104) for donor reconstitution, CD4-PerCP-Cy5 (BD Pharmingen RM-4, San Jose, CA, USA) and CD8-PE (eBioscience 53–6.7) for T lymphocytes, B220-PE-Cy5 (eBioscience RA3–6B2) or B220-PerCP-Cy5.5 (eBioscience RA3–6B2) and CD19-PE (eBioscience eBioD3) for B lymphocytes, or CD11b-PerCP-Cy5.5 (eBioscience M1/70) and Gr-1-PE (BD Pharmingen RB6.8C5) for myeloid cells.

Isolation of hematopoietic progenitors and FACS

BM cells were flushed from tibia and femur, treated with ACK to lyse RBCs, and filtered. Mature BM cells were lineage depleted with a standard cocktail of rat antibodies: CD2, CD3, CD5, CD8, CD11b, Ly-6G, TER119, CD45R, and CD19. Labeled cells were removed by two consecutive depletions with Dynabeads sheep antirat IgG (Invitrogen Dynal). Remaining progenitor cells were incubated with Sca-1-PE (BD Pharmingen D7) and c-Kit-AF647, and DAPI for viability. Cell data was collected with BD FACSAria or BD FACScanto II and data analysis was done with BD FlowJo software. Monoclonal antibodies raised against CD2 (Rm2.2), CD3 (KT3–1.1), CD5 (53–7.3), CD8 (53–6.7), CD11b (M1/70), Ly-6G (RB6–8C5), TER119, CD45R (RA3–6B2), CD19 (1D3), and c-Kit (3C11) were purified from cultured hybridomas.

Statistical analysis

Data are given as means ± standard deviation. Student's *t*-test was used to determine significant differences between samples.

Acknowledgments

The authors would like to thank members of both Weis labs for their insightful and stimulating critiques of this work. This work was supported by grants from the National Institute of Allergy and Infectious Diseases (AI-24158, JHW: AI-32223, JJW). The content is solely the responsibility of the authors and does not necessarily represent the official views of the Institute of Allergy and Infectious Diseases or the National Institutes of Health. T.J.D. was supported as a predoctoral trainee by NIH Genetics Training Grant T32-GM07464.

References

1. Hemavathy K, Ashraf SI, Ip YT. Snail/slug family of repressors: slowly going into the fast lane of development and cancer. Gene. 2000; 257:1–12. [PubMed: 11054563]
2. Nieto MA. The snail superfamily of zinc-finger transcription factors. Nat Rev Mol Cell Biol. 2002; 3:155–166. [PubMed: 11994736]
3. Kataoka H, Murayama T, Yokode M, Mori S, Sano H, Ozaki H, Yokota Y, et al. A novel snail-related transcription factor Smuc regulates basic helix-loop-helix transcription factor activities via specific E-box motifs. Nucleic Acids Res. 2000; 28:626–633. [PubMed: 10606664]
4. Peinado H, Del Carmen Iglesiasde la Cruz M, Olmeda D, Csiszar K, Fong KS, Vega S, Nieto MA, et al. A molecular role for lysyl oxidase-like 2 enzyme in snail regulation and tumor progression. Embo J. 2005; 24:3446–3458. [PubMed: 16096638]
5. Hale JS, Dahlem TJ, Margraf RL, Debnath I, Weis JJ, Weis JH. Transcriptional control of Pactolus: evidence of a negative control region and comparison with its evolutionary paralogue, CD18 (beta2 integrin). J Leukoc Biol. 2006; 80:383–398. [PubMed: 16735694]

6. Nakakura EK, Watkins DN, Schuebel KE, Sriuranpong V, Borges MW, Nelkin BD, Ball DW. Mammalian Scratch: a neural-specific Snail family transcriptional repressor. Proc Natl Acad Sci USA. 2001; 98:4010–4015. [PubMed: 11274425]
7. Jiang R, Lan Y, Norton CR, Sundberg JP, Gridley T. The Slug gene is not essential for mesoderm or neural crest development in mice. Dev Biol. 1998; 198:277–285. [PubMed: 9659933]
8. Murray SA, Gridley T. Snail family genes are required for left-right asymmetry determination, but not neural crest formation, in mice. Proc Natl Acad Sci USA. 2006; 103:10300–10304. [PubMed: 16801545]
9. Moreno-Bueno G, Cubillo E, Sarrio D, Peinado H, Rodriguez-Pinilla SM, Villa S, Bolos V, et al. Genetic profiling of epithelial cells expressing E-cadherin repressors reveals a distinct role for Snail, Slug, and E47 factors in epithelial-mesenchymal transition. Cancer Res. 2006; 66:9543–9556. [PubMed: 17018611]
10. Bolos V, Peinado H, Perez-Moreno MA, Fraga MF, Esteller M, Cano A. The transcription factor Slug represses E-cadherin expression and induces epithelial to mesenchymal transitions: a comparison with Snail and E47 repressors. J Cell Sci. 2003; 116:499–511. [PubMed: 12508111]
11. Perez-Losada J, Sanchez-Martin M, Rodriguez-Garcia A, Sanchez ML, Orfao A, Flores T, Sanchez-Garcia I. Zinc-finger transcription factor Slug contributes to the function of the stem cell factor c-kit signaling pathway. Blood. 2002; 100:1274–1286. [PubMed: 12149208]
12. Perez-Mancera PA, Perez-Caro M, Gonzalez-Herrero I, Flores T, Orfao A, de Herreros AG, Gutierrez-Adan A, et al. Cancer development induced by graded expression of Snail in mice. Hum Mol Genet. 2005; 14:3449–3461. [PubMed: 16207734]
13. Perez-Mancera PA, Gonzalez-Herrero I, Perez-Caro M, Gutierrez-Cianca N, Flores T, Gutierrez-Adan A, Pintado B, et al. SLUG in cancer development. Oncogene. 2005; 24:3073–3082. [PubMed: 15735690]
14. Cobaleda C, Perez-Caro M, Vicente-Duenas C, Sanchez-Garcia I. Function of the zinc-finger transcription factor SNAI2 in cancer and development. Annu Rev Genet. 2007; 41:41–61. [PubMed: 17550342]
15. Zhuge X, Kataoka H, Tanaka M, Murayama T, Kawamoto T, Sano H, Togi K, et al. Expression of the novel Snai-related zinc-finger transcription factor gene Smuc during mouse development. Int J Mol Med. 2005; 15:945–948. [PubMed: 15870897]
16. Newkirk KM, MacKenzie DA, Bakaletz AP, Hudson LG, Kusewitt DF. Microarray analysis demonstrates a role for Slug in epidermal homeostasis. J Invest Dermatol. 2008; 128:361–369. [PubMed: 17637818]
17. Katoh M. Identification and characterization of human SNAIL3 (SNAI3) gene in silico. Int J Mol Med. 2003; 11:383–388. [PubMed: 12579345]
18. Lagasse E, Weissman IL. Flow cytometric identification of murine neutrophils and monocytes. J Immunol Methods. 1996; 197:139–150. [PubMed: 8890901]
19. DeKoter RP, Singh H. Regulation of B lymphocyte and macrophage development by graded expression of PU.1. Science. 2000; 288:1439–1441. [PubMed: 10827957]
20. Xie H, Ye M, Feng R, Graf T. Stepwise reprogramming of B cells into macrophages. Cell. 2004; 117:663–676. [PubMed: 15163413]
21. Serwold T, Richie Ehrlich LI, Weissman IL. Reductive isolation from bone marrow and blood implicates common lymphoid progenitors as the major source of thymopoiesis. Blood. 2009; 113:807–815. [PubMed: 18927436]
22. van de Rijn M, Heimfeld S, Spangrude GJ, Weissman IL. Mouse hematopoietic stem-cell antigen Sca-1 is a member of the Ly-6 antigen family. Proc Nat Acad Sci USA. 1989; 86:4634–4638. [PubMed: 2660142]
23. Kondo M, Weissman IL, Akashi K. Identification of clonogenic common lymphoid progenitors in mouse bone marrow. Cell. 1997; 91:661–672. [PubMed: 9393859]
24. Kondo M, Scherer DC, King AG, Manz MG, Weissman IL. Lymphocyte development from hematopoietic stem cells. Curr Opin Genet Dev. 2001; 11:520–526. [PubMed: 11532393]
25. Ikuta K, Weissman IL. Evidence that hematopoietic stem cells express mouse c-kit but do not depend on steel factor for their generation. Proc Nat Acad Sci USA. 1992; 89:1502–1506. [PubMed: 1371359]

26. Perry SS, Pierce LJ, Slayton WB, Spangrude GJ. Characterization of Thymic Progenitors in Adult Mouse Bone Marrow. J Immunol. 2003; 170:1877–1886. [PubMed: 12574354]

27. Nakanishi T, Kuroiwa A, Yamada S, Isotani A, Yamashita A, Tairaka A, Hayashi T, et al. FISH analysis of 142 EGFP transgene integration sites into the mouse genome. Genomics. 2002; 80:564–574. [PubMed: 12504848]

28. Morita S, Kojima T, Kitamura T. Plat-E: an efficient and stable system for transient packaging of retroviruses. Gene Ther. 2000; 7:1063–1066. [PubMed: 10871756]

29. Yun TJ, Bevan MJ. Notch-regulated ankyrin-repeat protein inhibits Notch1 signaling: multiple Notch1 signaling pathways involved in T-cell development. J Immunol. 2003; 170:5834–5841. [PubMed: 12794108]

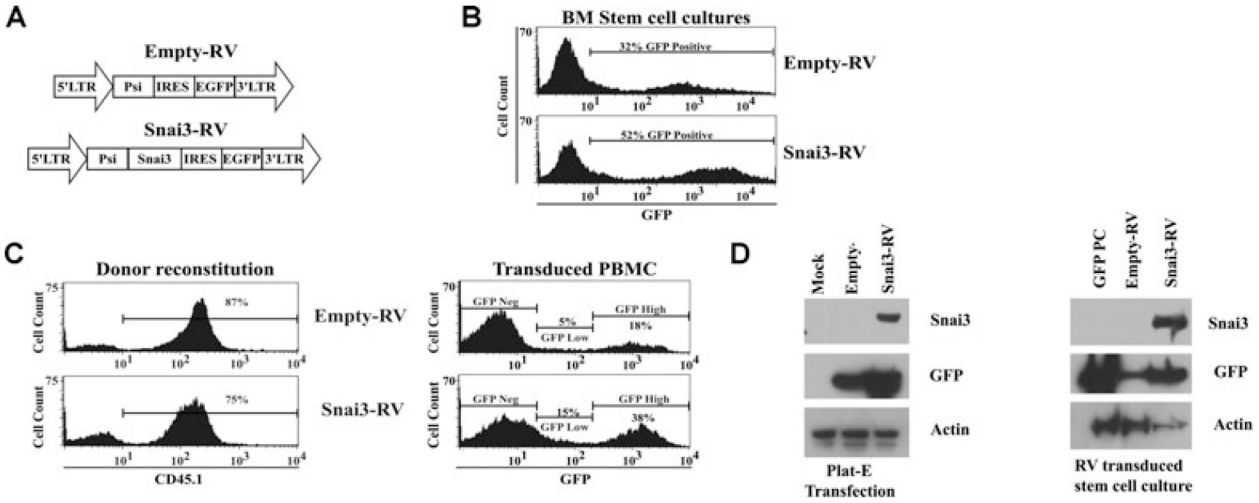

Figure 1.

Retroviral constructs plus transduction and reconstitution efficiency. (A) The pBMN-1-GFP retroviral plasmid is shown with the Snai3 coding sequence inserted upstream of the IRES for the GFP gene. (B) Histogram shows an example of BM cells transduced with RV based on GFP expression. (C) Histograms show donor lineage contribution in PBMCs of RV-chimeric mice (CD45.1, left) and percentage of PBMCs in chimeric mice containing RV by GFP expression (right). The GFP histogram was gated into three subsets: GFP^{-} (nontransduced), GFP^{low} (intermediate), and GFP^{High} (transduced) for further examination of PBMCs (right). (D) Immunoblots of lysates from Plat E virus-packing cell line transfected with mock, Empty-RV, or Snai3-RV constructs, probed with antibodies specific for GFP, β-actin and Snai3 (left), and of BM stem cell cultures transduced with the Empty-RV or Snai3-RV retrovirus constructs (right). As a positive control, BM from the ROSA-GFP transgenic mouse, with constitutive GFP expression, was used (GFP PC). (B–D) represent data taken from one set of infections and transfers, however, they are representative of more than three similar analyses

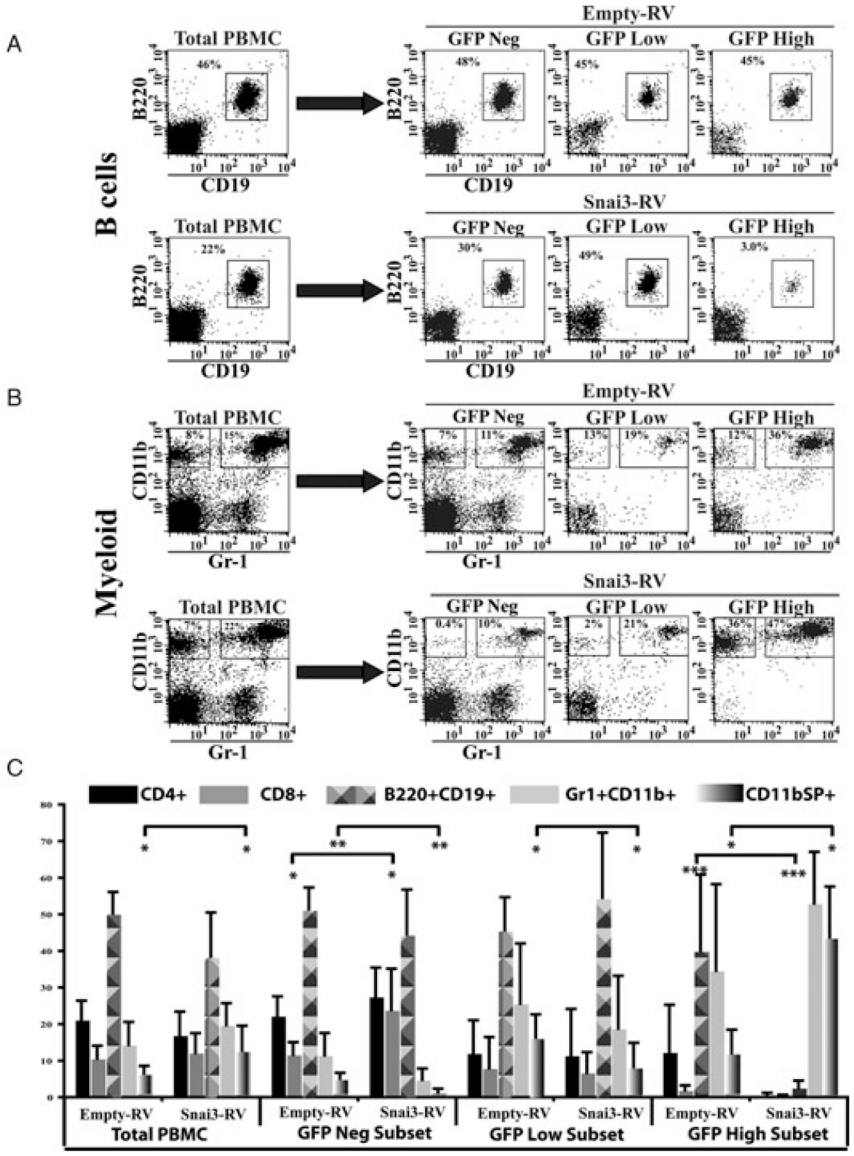

Figure 2.

Analysis of RV-chimeric mice PBMCs for hematopoietic lineages. Lineage analysis of PBMCs for B-cell and myeloid lineages using standard surface markers on gated GFP subsets (See Fig. 1C). Total PBMC lineage populations are shown at the left and each gated subset is shown on the right. (A) B lymphocyte analysis using B220 and CD19 markers. (B) Myeloid analysis using Gr-1 and CD11b. Percentiles denote cells within that gate compared with total cells within that plot. (C) Statistical analysis of 12 weeks PBMC populations from Empty-RV ($n = 9$) and Snai3-RV ($n = 7$) chimeric mice analyzed on three different dates. Data are shown as mean + SD; *statistically significant difference in a defined lineage when comparing Snai3-RV with Empty-RV mice within each gated subset. All p-values ≤ 0.03 with a majority of p-values ≤ 0.007. $CD4^+$ and $CD8^+$: T cells, $B220^+/CD19^+$: B cells. $Gr1^+CD11b^+$: granulocytes, CD11bSP: monocytes.

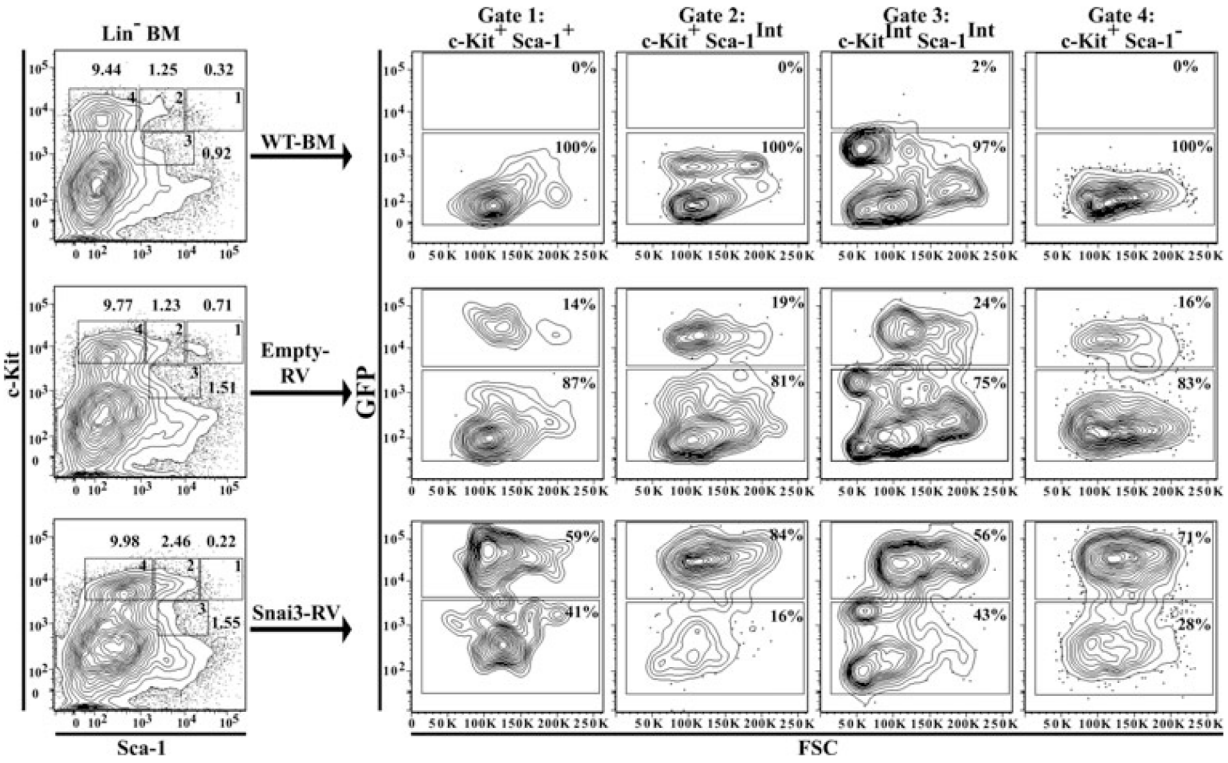

Figure 3.

Analysis of HSC progenitor cells. Data shown are obtained from representative animals for both Empty-RV and Snai3-RV mice but are similar to that obtained from an additional four animals per chimera model. Lin^- BM was gated into four subpopulations based on c-Kit and Sca-1 staining (left). Numbers next to each gate represent the percentage of cells in each gate. Each subpopulation (Gate 1–4) was separated into GFP^+ (top box) and GFP^- (bottom box) populations versus forward scatter. The number in each box represents the percentage of the gated subpopulation. GFP^+ cell were found in each subpopulations for both GFP-RV and Snai3-RV mice. The data plots shown are from one set of analyses and are representative of three distinct experiments.